Experimental continuation in nonlinear dynamics: recent advances and future challenges - Supplementary material

Ghislain Raze, Gaëtan Abeloos and Gaëtan Kerschen

[*]Aerospace and Mechanical Engineering Department, University of Liège, Allée de la Découverte, 9, Liège, 4000, Belgium.

*Corresponding author(s). E-mail(s): g.raze@uliege.be;

1 Introduction

This document gathers supplementary information for the manuscript "Control-based nonlinear vibration testing". Detailed descriptions of the experimental setups, namely an electronic Duffing oscillator and a clamped plate, are given in Section 2 and 3, respectively. The complete list of parameters used in the different methods are given in Section 4. Section 5 discusses the implementation details of some methods. Finally, Section 6 explains how Gaussian process regression has been performed on the measured data.

2 Details about the electronic Duffing oscillator

The electronic Duffing oscillator used in this work follows the schematics given in Figure 1, inspired from [1, 2]. The response x of this oscillator to an external excitation f is theoretically governed by the following ordinary differential equation:

$$m\ddot{x}(t) + c\dot{x}(t) + kx(t) + k_3x^3(t) = f(t), \tag{1}$$

where m, c, k and k_3 are the mass, damping coefficient, linear stiffness and cubic stiffness coefficient, respectively, and an overdot denotes a derivation with respect to time t.

Assuming ideal operational amplifier and analog multiplier behaviors, and neglecting the loading effects of the potentiometers on the summing amplifier, this circuit

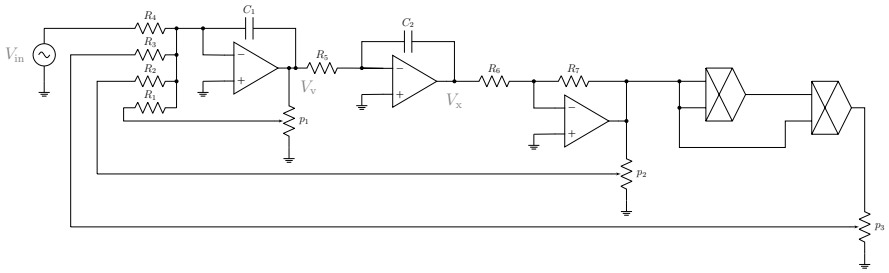

Fig. 1: Schematics of the electronic Duffing oscillator.

can be shown to be governed by the following ordinary differential equation:

$$C_1 C_2 R_4 R_5 \ddot{V}_\mathrm{x} + p_1 \frac{C_2 R_4 R_5}{R_1} \dot{V}_\mathrm{x} + p_2 \frac{R_4 R_7}{R_2 R_6} V_\mathrm{x} + p_3 \frac{g_m^2 R_4 R_7^3}{R_3 R_6^3} V_\mathrm{x}^3 = V_\mathrm{in}, \tag{2}$$

where V_in and V_x are the input and output voltages of the circuit, respectively, R_n are resistances, C_n are capacitances, p_n are voltage division ratios associated with potentiometers, and g_m is the analog multiplier's gain. Identifying V_in and V_x to f and x in Equation (1), Equation (2) is indeed verified to be of the form of Duffing's equation. The output of the first operational amplifier was also monitored, and is related to the time derivative of V_x through

$$V_\mathrm{v} = -C_2 R_5 \dot{V}_\mathrm{x}, \tag{3}$$

as V_v and V_x are the input and output of an integrator, respectively. The values of all electrical parameters for this study are given in Table 1. More details about this electronic circuit can be found in [3].

Table 1: Electrical parameters of the electronic Duffing oscillator.

Parameter	Value
R_1 (kΩ)	100
R_2 (kΩ)	10
R_3 (kΩ)	1
R_4 (kΩ)	100
R_5 (kΩ)	1
R_6 (kΩ)	10
R_7 (kΩ)	10
C_1 (μF)	1
C_2 (μF)	1
g_m (V^{-1})	0.1

Measurements on the board allowed to determine the potentiometer parameters as $p_1 = 0.1311$, $p_2 = 0.1923$ and $p_3 = 0.9887$. Comparing Equations (1) and (2), the parameters given in Table 2 were thus found for the Duffing oscillator. The parameters were also computed with the frequency subspace nonlinear system identification method [4] with data from one of the swept-sine tests. The main discrepancies with the experimentally identified values are in line with the various uncertainties on the capacitances (5%), as well as the inaccuracies due to the fact that the circuit does not exactly respect the aforementioned idealizations.

Table 2: Theoretical and identified parameters of the electronic Duffing oscillator.

Parameter	Theoretical value	Identified value
m (s^2)	10^{-4}	1.0461×10^{-4}
c (s)	$1.3{\times}10^{-4}$	$1.4231{\times}10^{-4}$
k (-)	1.923	1.8099
k_3 (V^{-2})	0.9887	1.0077

3 Details about the clamped plate

Figure 2 schematizes the experimental clamped plate setup.

The 500 mm × 300 mm × 0.5 mm stainless steel plate was purchased from RS (with reference 559-206). The clamping device is a Tecuro SKON3840600 38/40 × 600 mm × 2 mm Galvanised Steel C/U Profile. Seven holes (evenly spaced by 40 mm) were drilled in each side (12.5 mm away from the edge) of the plate to fix it to the clamping arms with M5 bolts and washers of 30 mm diameter. The lower edge of the plate is 65 mm away higher than the optical table. The transverse stiffening bar (to improve midplane stretching effects) was made of two L-shaped profiles of 300 mm length with 40 mm sides of 2mm thickness, which are bolted to the cantilever arms 60 mm above the plate upper edge. The distance between the two clamping devices (also corresponding to the clamped plate span) is 437 mm.

The plate was excited with an electrodynamic shaker (TIRA TV 51075) in current mode, and the response of the plate was monitored with an impedance head (DYTRAN 5860B) as well as a laser vibrometer (Polytec NLV-2500-5). The laser measurement point is located at 125 mm lengthwise and 20 mm widthwise from the top left corner, whereas the impedance head is glued at 60 mm lengthwise and 60 mm widthwise from the lower left corner.

4 Parameters

This section gathers all parameters used during the experiments.

4.1 Electronic Duffing oscillator

We start with the parameters for the primary and superharmonic resonances of the Duffing oscillator. We note that for CBC methods, the gain k_d is defined with the

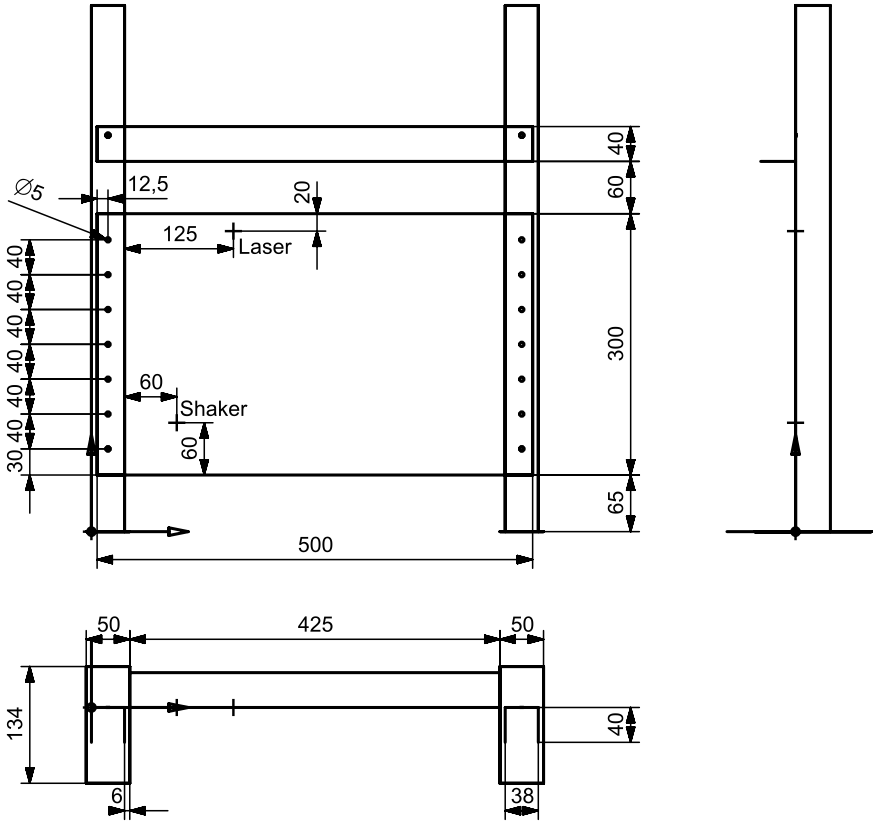

Fig. 2: Detailed schematics of the clamped plate setup (all dimensions are in mm).

feedback law using the velocity signal

$$V_{\mathrm{in}}(t) = -k_{\mathrm{d}}(x_*(t) - V_{\mathrm{v}}(t)), \tag{4}$$

and, recalling with Equation (3) and Table 1 that $V_{\mathrm{v}} = -10^{-3}V_{\mathrm{x}}$, an equivalent direct velocity feedback coefficient would thus be $10^{-3}k_{\mathrm{d}}$.

4.1.1 Primary resonance

Table 3 gathers the parameters common to all tests of the primary resonance of the electronic Duffing oscillator, whereas Tables 4, 5, 6, 7 and 8 contain the parameters specific to the CBC-FD, SCBC, PLL, RCT and ACBC methods, respectively.

Table 3: Common parameters for the primary resonance of the electronic Duffing oscillator.

Parameter	Value
t_s (s)	10^{-4}
t_{steady} (s)	0.5
$\bar{\mu}$ (-)	0.5
h (-)	5

Table 4: Parameters of the CBC-FD method for the primary resonance of the electronic Duffing oscillator.

Parameter	Value
k_{d} (-)	10
$\Delta\lvert V_{\text{v}}\rvert_1$ (V)	0.01
$\Delta\omega$ (rad s^{-1})	5
ρ (-)	0.05

Table 5: Parameters of the SCBC method for the primary resonance of the electronic Duffing oscillator.

Parameter	Value
k_{d} (-)	10
$\Delta\lvert V_{\text{v}}\rvert_1$ (V)	0.01
$\Delta\omega$ (rad s^{-1})	5
ρ (-)	0.05 (Picard)
ρ (-)	0.01 (Adaptive filters)

Table 6: Parameters of the PLL method for the primary resonance of the electronic Duffing oscillator.

Parameter	Value
$d\theta_*/dt$ (rad s^{-1})	-0.013
k_{p} (s^{-1})	20
k_{i} (s^{-2})	10

Table 7: Parameters of the RCT method for the primary resonance of the electronic Duffing oscillator.

Parameter	Value
$\Delta\lvert V_\mathrm{x}\rvert_1$ (V)	0.06
$\Delta\omega$ (rad s^{-1})	5
Number of periods (-)	5
Confidence	Low
FRF error correction (%)	50
Max. control iter. (-)	10
Max. drive update (%)	20
Max. amplitude var. (%)	20
Delay (cycles)	0

Table 8: Parameters of the ACBC method for the primary resonance of the electronic Duffing oscillator.

Parameter	Value
k_d (-)	10
$\Delta\lvert V_\mathrm{v}\rvert_1$ (V)	0.01
$\Delta\omega$ (rad s^{-1})	5
ρ (-)	0.01
σ (-)	0.5
k_α (rad s^{-1} V^{-1})	10

4.1.2 3:1 superharmonic resonance

Table 9 gathers the parameters common to all tests of the 3:1 superharmonic resonance of the electronic Duffing oscillator, whereas Tables 10, 11 and 12 contain the parameters specific to the CBC-FD, PLL and ACBC methods, respectively.

Table 9: Common parameters for the 3:1 superharmonic resonance of the electronic Duffing oscillator.

Parameter	Value
t_s (s)	10^{-4}
t_steady (s)	0.5
$\bar{\mu}$ (-)	0.25
h (-)	9

Table 10: Parameters of the CBC-FD method for the 3:1 superharmonic resonance of the electronic Duffing oscillator.

Parameter	Value
k_d (-)	50
$\Delta\lvert V_\mathrm{v}\rvert_1$ (V)	0.01
$\Delta\omega$ (rad s^{-1})	0.2
ρ (-)	0.01

Table 11: Parameters of the PLL method for the 3:1 superharmonic resonance of the electronic Duffing oscillator.

Parameter	Value
$d\theta_*/dt$ (rad s^{-1})	-0.013
k_p (s^{-1})	10
k_i (s^{-2})	5

Table 12: Parameters of the ACBC method for the 3:1 superharmonic resonance of the electronic Duffing oscillator.

Parameter	Value
k_d (-)	50
$\Delta\lvert V_\mathrm{v}\rvert_1$ (V)	0.01
$\Delta\omega$ (rad s^{-1})	0.2
ρ (-)	0.01
σ (-)	0.5
k_α (rad s^{-1} V^{-1})	10

4.2 Clamped plate

Details are now given about the parameters used for the clamped plate setup.

In addition to the repeatability issues mentioned in the article, the clamped plate set-up also has a feature that makes it not completely reproducible. This is due to the shaker amplifier gain knob that can continuously be varied. Between different tests, it was moved as little as possible, but some operations made it mandatory to set the knob gain to zero, and then back as close as possible to its previous position. From the measured FRFs, a static gain of approximately 6.3 N/V and 0.72 A/V was identified to correspond to this knob position.

Table 13 gathers the parameters common to all tests of the clamped plate oscillator, whereas Tables 14, 15 and 16 contain the parameters specific to the SCBC, PLL and ACBC methods, respectively. We also recall that a low-pass filter with transfer function

$$H_{\mathrm{lp}}(p) = \frac{1}{p/(2\pi f_{\mathrm{lp}}) + 1} \tag{5}$$

was applied to the sensed signal (where p is Laplace's variable and $f_{\mathrm{lp}} = 500$ Hz is the filter's cut-off frequency).

Table 13: Common parameters for the clamped plate.

Parameter	Value
t_s (s)	10^{-4}
t_{steady} (s)	0.5
$\bar{\mu}$ (-)	0.5
h (-)	15

Table 14: Parameters of the SCBC method for the clamped plate.

Parameter	Value
k_{d} (-)	2.5
$\Delta\lvert V_{\mathrm{v}}\rvert_1$ (V)	0.05
$\Delta\omega$ (rad s^{-1})	0.5
ρ (-)	0.01

Table 15: Parameters of the PLL method for the clamped plate.

Parameter	Value
$d\theta_*/dt$ (rad s^{-1})	–0.0164
k_{p} (s^{-1})	20
k_{i} (s^{-2})	10

Table 16: Parameters of the ACBC method for the clamped plate.

Parameter	Value
k_d (-)	2.5
$\Delta\lvert V_\mathrm{v}\rvert_1$ (V)	0.05
$\Delta\omega$ (rad s^{-1})	0.5 (Mode 2)
$\Delta\omega$ (rad s^{-1})	1 (Broadband)
ρ (-)	0.01
σ (-)	0.5
k_α (rad s^{-1} V^{-1})	100

5 Implementation details

We give some details about the implementation of different methods, namely CBC-FD, RCT, PLL for phase resonance tracking, and CBC fold bifurcation tracking.

5.1 CBC-FD

A fully online implementation of the CBC-FD method was used in this work. The method works with a constant scaling of the variables based on $\Delta\lvert V_\mathrm{v}\rvert_1$ and $\Delta\omega$ for the Fourier coefficients and frequency, respectively. In these scaled variables, the norm of the prediction is equal to one.

A quasi-Newton-chord method was used for the corrections. The Jacobian is evaluated with finite differences after a given number of successful prediction, and updated with Broyden's formula, similarly to, e.g., [5]. Corrections $\Delta\mathbf{x}$ obtained from a pseudo-arclength corrector are limited based on the unknowns vector $\mathbf{x}$ if they exceed a certain fraction of the latter in norm, i.e., from $\Delta\mathbf{x}$ the effective correction is $(\Delta\mathbf{x})_\mathrm{QN}$ given by

$$(\Delta\mathbf{x})_\mathrm{QN} = \begin{cases} \Delta\mathbf{x} & \text{if } ||\Delta\mathbf{x}|| \leq \gamma||\mathbf{x}|| \\ \gamma||\mathbf{x}||\Delta\mathbf{x}/||\Delta\mathbf{x}|| & \text{if } ||\Delta\mathbf{x}|| > \gamma||\mathbf{x}|| \end{cases} . \tag{6}$$

If the number of corrections exceeds a predefined threshold, the correction procedure is stopped and the Jacobian is reevaluated with finite differences (it was however noted that this procedure was triggered when the algorithm had convergence trouble, and seldom helped to retrieve a convergent behavior). The parameters of the CBC-FD method used in this work are gathered in Table 17.

Table 17: Parameters of the CBC-FD method.

Parameter	Value
Finite difference step (-)	0.05
γ (-)	0.2
Steps for Jacobian evaluation (-)	5
Max. number of corrections (-)	10

5.2 RCT

The nominal parameters for the RCT given in Table 7 were chosen heuristically. We also tried to vary these nominal parameters in an attempt to suppress the instability issues, as given in Table 18 (where parameters highlighted in red indicate the difference with the nominal case). To avoid long tests, these parameters were tried out with a target amplitude meeting the unstable zone when the frequency is varied with steps of 1 Hz, namely $a_* = 0.5$ V, with a relative tolerance of $\rho = 0.01$ on the amplitude. Figure 3 shows the resulting harmonic amplitude spectrum; clearly, instabilities appear for all the investigated cases.

Table 18: Parameters for the parametric study of the RCT method in TestLab.

Parameter	Value 1	Value 2	Value 3	Value 4	Value 5	Value 6
Number of periods (-)	5	5	1	2	10	5
Confidence	Medium	High	Low	Low	Low	Low
FRF error correction (%)	50	50	50	50	50	50
Max. control iter. (-)	10	10	10	10	10	10
Max. drive update (%)	20	20	20	20	20	50
Max. amplitude var. (%)	20	20	20	20	20	20
Delay (cycles)	0	0	0	0	0	0

Parameter	Value 7	Value 8	Value 9	Value 10	Value 11	Value 12
Number of periods (-)	5	5	5	5	5	5
Confidence	Low	Low	Low	Low	Low	Low
FRF error correction (%)	50	50	25	100	50	50
Max. control iter. (-)	10	10	10	10	5	20
Max. drive update (%)	20	50	20	20	20	20
Max. amplitude var. (%)	50	50	20	20	20	20
Delay (cycles)	0	0	0	0	0	0

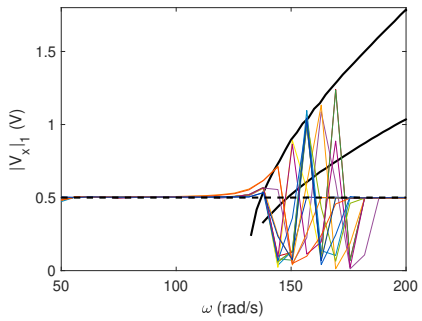

Fig. 3: Parametric study for the RCT: harmonic displacement amplitude with $a_* = 0.5$ V. The thin colored lines represent the tests with the parameters of Tables 7 and 18, the thick dashed line is the target harmonic amplitude (a_*), and the thick full lines are the loci of fold bifurcations.

5.3 PLL for phase resonance tracking

Table 19: Parameters of the PLL method for the 1:1 phase resonance tracking.

Parameter	Value
$\bar{\mu}$ (-)	0.5
θ_1 (rad)	$-\pi/2$
df/dt (V s^{-1})	10^{-3}

Table 20: Parameters of the PLL method for the 2:1 phase resonance tracking.

Parameter	Value
$\bar{\mu}$ (-)	0.25
θ_2 (rad)	0
df/dt (V s^{-1})	5×10^{-2}

Table 21: Parameters of the PLL method for the 3:1 phase resonance tracking.

Parameter	Value
$\bar{\mu}$ (-)	0.16
θ_3 (rad)	$-\pi/2$
df/dt (V s^{-1})	2×10^{-2}

The PLL allows for an easy implementation of phase resonance tracking, both for primary [6, 7] and secondary [8] resonances. The main difference with the NFR measurement is that θ is fixed, and f is varied. In addition, secondary resonances consider the phase of the resonant harmonic (instead of that of the fundamental harmonic), which can easily be deduced from the Fourier decomposition of the response. Tables 19, 20 and 21 gather the parameters associated with the 1:1, 2:1 and 3:1 phase resonance tracking procedures, respectively; the remaining parameters are identical to those gathered in Tables 3 and 6.

5.4 CBC fold bifurcation tracking

The experimental fold bifurcation tracking procedure implemented in this work follows the method explained in [9], which is based on finding an extremum of a fitted (a, f)

curve for different values of ω. The implementation used in this work started from an interval of width $2\Delta a$, centered around an initial guess a_0 of the amplitude of the fold at the considered frequency. If the minimum was within $0.01\Delta a$ of the center of the interval, that point was accepted as an estimate of the fold and the frequency was changed by a step $\Delta\omega$. If the minimum was within $0.25\Delta a$ of the center of the interval, the interval was recentered around the estimated location of the fold and narrowed using $\Delta a \rightarrow 0.5\Delta a$. Finally, if neither of these conditions were met but the fold was estimated to be inside the interval, this interval was recentered (without narrowing) around the estimated value; the procedure was stopped otherwise. As in [9], two sequential continuations were needed for the upper and lower fold branches. In our implementation for the electronic Duffing oscillator, we used $\Delta a = 0.02$ V and $\Delta\omega = -2.5$ rad/s. The remaining parameters of the method are given in Table 3.

6 Gaussian process regression

Gaussian process regression (GPR) is a powerful tool to solve probabilistic regression problems. It was thus expected to be useful to interpret the repeatability tests. However, these processes consider that the observables can be expressed as the sum of functions of some variables (predictors) and a Gaussian noise with constant variance. Clearly, this cannot be applied directly to folded curves with variable noise. This section explains the step followed to apply GPR to our problem, inspired from [10].

6.1 Regression with cubic splines

A first step was to find adequate predictors for the point cloud resulting from a series of repeatability tests. This point cloud can easily be interpreted as a noisy curve by a human, but is harder to treat with a computer. To enable the use of GPR, we fitted the point cloud with a smooth curve, in this case a piecewise-cubic spline with ten segments. The number of segments was chosen heuristically, to provide a sufficiently geometrically accurate description of the cloud point, all the while avoiding overfitting. The control points of the spline were first graphically determined using the `ginput` function from Matlab. They were then optimized using a nonlinear least-squares optimizer (`fminunc`).

6.2 Gaussian process regression with local coordinates

Thanks to the backbone formed by the spline, it was possible to express each point of the point cloud with a unique predictor (for a given spline). To do that, we projected each point orthogonally on the curve to find its tangential coordinate, giving an abscissa for the GPR. The ordinate was then found as the signed distance to the curve along its normal. These tangential and normal coordinates, hereafter called "local coordinates", were finally used in the GPR. Since the spline has a piecewise polynomial representation, it was possible to find these coordinates semi-analytically with the `roots` function.

A first GPR was performed to compute the average of the point cloud along the spline with the function `fitrgp`. By retransforming the local coordinates into global

ones, it was thus possible to visualize the mean curve fitting the point cloud (which generally was close to the spline but could capture smaller-scale features).

This GPR also provided a confidence interval, but this interval was seen to be almost constant along the curve, giving little information about the spread of the point cloud. To refine this information, a second GPR fitting the square of the difference between the point cloud and its GPR (in local coordinates) was performed to capture the variance of the process. By adding or subtracting the square root of this new GPR times an adequate factor, a variable confidence interval was thus captured.

References

[1] Jones, B.K., Trefan, G.: The Duffing oscillator: A precise electronic analog chaos demonstrator for the undergraduate laboratory. American Journal of Physics **69**(4), 464–469 (2001) https://doi.org/10.1119/1.1336838

[2] Srinivasan, K., Thamilmaran, K., Venkatesan, A.: Effect of nonsinusoidal periodic forces in Duffing oscillator: Numerical and analog simulation studies. Chaos, Solitons & Fractals **40**(1), 319–330 (2009) https://doi.org/10.1016/j.chaos.2007.07.090

[3] Raze, G.: An electronic Duffing oscillator (2024). https://github.com/GhislainRaze/Electronic-Duffing

[4] Noël, J.P., Kerschen, G.: Frequency-domain subspace identification for nonlinear mechanical systems. Mechanical Systems and Signal Processing **40**(2), 701–717 (2013) https://doi.org/10.1016/j.ymssp.2013.06.034

[5] Bureau, E.: Experimental bifurcation analysis using control-based continuation. PhD thesis, Technical University of Denmark (2014). https://findit.dtu.dk/en/catalog/53be7cc5f7d9a21b490001de

[6] Peter, S., Leine, R.I.: Excitation power quantities in phase resonance testing of nonlinear systems with phase-locked-loop excitation. Mechanical Systems and Signal Processing **96**, 139–158 (2017) https://doi.org/10.1016/j.ymssp.2017.04.011

[7] Scheel, M., Peter, S., Leine, R.I., Krack, M.: A phase resonance approach for modal testing of structures with nonlinear dissipation. Journal of Sound and Vibration **435**, 56–73 (2018) https://doi.org/10.1016/j.jsv.2018.07.010 arXiv:2011.08500

[8] Zhou, T., Kerschen, G.: Identification of secondary resonances of nonlinear systems using phase-locked loop testing. Journal of Sound and Vibration, 118549 (2024) https://doi.org/10.1016/j.jsv.2024.118549

[9] Renson, L., Barton, D.A.W., Neild, S.A.: Experimental tracking of limit-point bifurcations and backbone curves using control-based continuation. International

Journal of Bifurcation and Chaos **27**(1), 1–19 (2017) https://doi.org/10.1142/S0218127417300026

[10] Goldberg, P.W., Williams, C.K.I., Bishop, C.M.: Regression with input-dependent noise a gaussian process treatment. Advances in Neural Information Processing Systems, 493–499 (1998)